Many-Body Problem in Quantum Statistical Mechanics. III. Zero-Temperature Limit for Dilute Hard Spheres*

T. D. LEE, *Columbia University, New York, New York*

AND

C. N. YANG, *Institute for Advanced Study, Princeton, New Jersey*

(Received June 17, 1959)

Using the method developed in paper I of this series, the thermodynamical properties at $T=0$ of a dilute system of hard spheres are computed for small values of ρa^3, where a is the diameter of the spheres and ρ is the particle density.

WE study in this paper the thermodynamical properties of a system of hard spheres at $T=0$. We recall that at a finite temperature T the pressure p depends on the chemical potential μ and on T. The thermodynamical relation,

$$dp=\rho d\mu+(S/\Omega)dT,$$

enables one to compute the density ρ and the entropy density (S/Ω) of the system. Once p is known as a function of μ and T, all other thermodynamical quantities can be calculated.

In Sec. I it will be shown that for a Fermi gas of hard spheres, using the results[1] of paper II, one can compute p at $T=0$ as a series involving successively higher powers of $\mu^{\frac{1}{2}}a$. From this expression one obtains the other thermodynamical properties of the system, such as the particle density ρ and the energy density. The energy density so obtained clearly represents the ground-state energy per unit volume. It is expressed in an asymptotic form valid for small values of $P_F a$, where P_F is the maximum Fermi momentum for free particles.

The corresponding calculation of p at fixed μ and at $T=0$ is more difficult for a Bose gas of hard spheres. The origin of the difficulty lies in the well known Bose-Einstein condensation which makes it difficult to take the limit $T\to 0$. In this paper we circumvent this difficulty by making the calculation for a Boltzmann gas of hard spheres, which does not exhibit a transition, and remark that at $T=0$ the thermodynamical properties of a Boltzmann gas are the same as that of a Bose gas. The calculation is outlined and summarized in Sec. 2, the mathematical details being given in the remaining sections of this paper.

1. FERMI STATISTICS

In this section[1] we calculate the pressure at $T=0$ at an arbitrary chemical potential μ for a Fermi system of hard spheres with spin J, to the order a^2. One first writes down the fugacity series (II.35) computed in paper II for finite T:

$$\lambda^3(p/\kappa T)=\lambda^3\sum_1^\infty b_l{}^A z^l$$
$$=-(2J+1)g_{\frac{5}{2}}(-z)-2J(2J+1)[g_{\frac{3}{2}}(-z)]^2(a/\lambda)$$
$$-8J^2(2J+1)g_{\frac{1}{2}}(-z)[g_{\frac{3}{2}}(-z)]^2(a/\lambda)^2$$
$$+8J(2J+1)F(-z)(a/\lambda)^2+0(a^3/\lambda^3), \quad \text{(III.1)}$$

where

$$g_n(z)=\sum_{l=1}^\infty l^{-n}z^n, \quad \text{(III.2)}$$

and

$$F(z)=\sum_{r,s,t=1}^\infty (rst)^{-\frac{1}{2}}(r+s)^{-1}(r+t)^{-1}z^{r+s+t}. \quad \text{(III.3)}$$

One recalls that according to the general principles of statistical mechanics, the fugacity z is related to the chemical potential μ by

$$z=\exp(\mu/\kappa T). \quad \text{(III.4)}$$

For fixed $\mu>0$, as $T\to 0$, clearly $z\to+\infty$. Equation (III.1) enables one to compute thel imit of p in successive approximations. In this computation the asymptotic limits of the functions $g_{\frac{5}{2}}$, $g_{\frac{3}{2}}$, $g_{\frac{1}{2}}$, and F are needed for arguments $(-z)\to-\infty$. In Appendix A these asymptotic limits are derived. Using these limits one obtains, as $T\to 0$, for fixed $\mu>0$,

$$(p)_{T=0}=(2J+1)(15\pi^2)^{-1}\mu^{\frac{5}{2}}-2J(2J+1)(9\pi^3)^{-1}a\mu^3$$
$$+4J(2J+1)\pi^{-4}[(2J/9)$$
$$-(11-2\ln 2)(105)^{-1}]a^2\mu^{7/2}+\cdots. \quad \text{(III.5)}$$

The form of this expression suggests that the higher order terms contain higher powers of $a\mu^{\frac{1}{2}}$. For finite but small values of T, the next order terms in the asymptotic expressions for the g functions contribute to the pressure p additional terms proportional to T^2, as can be easily verified with the aid of (III.62), (III.63), and (III.64).

The particle density and the energy density at $T=0$

* Work supported in part by the U. S. Atomic Energy Commission.

[1] T. D. Lee and C. N. Yang, Phys. Rev. **113**, 1165 (1959), and **116**, 25 (1959), referred to as I and II. We follow the notations of these papers. Thus p=pressure, $\hbar=1$, m=mass of particles$=\frac{1}{2}$, a=hard sphere diameter, N=number of particles, Ω=volume of box, $\rho=N/\Omega$, J=spin of particles, P_F=maximum Fermi momentum for free particles$=[6\pi^2\rho/(2J+1)]^{\frac{1}{3}}$, $\beta=1/\kappa T$, and $\lambda=(4\pi\beta)^{\frac{1}{2}}$.

for fixed $\mu>0$ are easily obtained from (III.5):

$$(\rho)_{T=0}=\frac{d}{d\mu}(p)_{T=0}=(2J+1)(6\pi^2)^{-1}\mu^{\frac{3}{2}} -2J(2J+1)(3\pi^3)^{-1}a\mu^2+14J(2J+1)\pi^{-4} \times[(2J/9)-(11-2\ln 2)(105)^{-1}]a^2\mu^{\frac{5}{2}} +\cdots, \quad \text{(III.6)}$$

$$(E/\Omega)_{T=0}=\mu\frac{d}{d\mu}(p)_{T=0}-(p)_{T=0}=(2J+1)(10\pi^2)^{-1}\mu^{\frac{5}{2}} -4J(2J+1)(9\pi^3)^{-1}a\mu^3+10J(2J+1)\pi^{-4} \times[(2J/9)-(11-2\ln 2)(105)^{-1}]a^2\mu^{7/2} +\cdots. \quad \text{(III.7)}$$

One can solve (III.6) for $\mu^{\frac{1}{2}}$:

$$\mu^{\frac{1}{2}}=P_F+4J(3\pi)^{-1}aP_F^2 -\left[\frac{8J^2}{9\pi^2}-\frac{4J}{\pi^2}\frac{(11-2\ln 2)}{15}\right]a^2P_F^3+\cdots. \quad \text{(III.8)}$$

Substituting this into (III.7) and dividing by ρ, one obtains the ground-state energy per particle:

$$(E/N)_{T=0}=(3P_F^2/5)+8\pi a\rho J(2J+1)^{-1} \times[1+6(11-2\ln 2)P_Fa(35\pi)^{-1}]+\cdots. \quad \text{(III.9)}$$

The result (III.9) was quoted some time ago in a short summary.[2] This result agrees with that obtained earlier from the pseudopotential method.[3]

2. BOLTZMANN STATISTICS (AND BOSE STATISTICS)

In a Boltzmann system, to approach the limit $T\to 0$ at fixed $\mu>0$ one must study the properties of p for values of the fugacity $z=\exp(\mu/\kappa T)\to+\infty$. This means that one must take into account all terms in the fugacity expansion $\sum b_lz^l$ and not cut off the series at any finite l. With this in mind we approach the problem in the following way: We calculate, for each l, the dominant terms in b_l for small values of a. These dominant terms have the following form:

$$b_l=\lambda^{-3}[\gamma_l(a/\lambda)^{l-1}+\delta_l(a/\lambda)^l+\cdots]. \quad \text{(III.10)}$$

The coefficients γ_l and δ_l are pure numbers. One defines the generating functions

$$\Gamma(x)=\sum_1^\infty \gamma_l(x/2)^l, \qquad \Delta(x)=\sum_1^\infty \delta_l(x/2)^l. \quad \text{(III.11)}$$

The coefficients γ_l and δ_l are computed in Secs. 3, 4, and 5, where one obtains explicit expressions for these generating functions Γ and Δ. Before discussing the physical consequences we first state the mathematical results of these computations. It will be shown that

$$\Gamma(x)=\tfrac{1}{2}D(x)+\tfrac{1}{4}[D(x)]^2, \quad \text{(III.12)}$$

where $D(x)$ is defined by

$$De^D=x. \quad \text{(III.13)}$$

It will be further shown in Secs. 4 and 5 that

$$\Delta(x)=\sum_{\mu=3}^\infty c_\mu(2\mu)^{-1}[-D(x)]^\mu, \quad \text{(III.14)}$$

where

$$c_\mu=2(\pi^{-\frac{1}{2}})\int_0^\infty q^{\frac{1}{2}}dq \int_{1\geqq t_\alpha\geqq 0} dt_1\cdots dt_\mu \times\exp\{-q[(t_{12}-t_{12}^2)+(t_{23}-t_{23}^2) +\cdots+(t_{\mu 1}-t_{\mu 1}^2)]\}, \quad \text{(III.15)}$$

and

$$t_{12}=|t_1-t_2|, \quad \text{etc.} \quad \text{(III.16)}$$

The function $D(x)$ in (III.14) was already defined in (III.13).

The pressure is expressible in terms of the generating functions, as a direct consequence of (III.10) and (III.11):

$$p=\sum_1^\infty b_lz^l=4\pi(a\lambda^4)^{-1}\Gamma(x)+4\pi\lambda^{-5}\Delta(x)+\cdots, \quad \text{(III.17)}$$

where

$$x=2az/\lambda=2a\lambda^{-1}\exp[\mu\lambda^2(4\pi)^{-1}]. \quad \text{(III.18)}$$

For fixed $\mu>0$, as $T\to 0$, $x\to+\infty$. Thus by (III.13) $D\to+\infty$. In fact, comparing (III.13) and (III.18) one obtains

$$D\to(4\pi)^{-1}\mu\lambda^2. \quad \text{(III.19)}$$

It is clear from (III.12) that

$$\Gamma(x)\to\tfrac{1}{4}D^2=(64\pi^2)^{-1}\mu^2\lambda^4. \quad \text{(III.20)}$$

The behavior of Δ as $D\to\infty$ can be studied from the explicit formulas (III.14)–(III.16). This is carried out in Appendix B where it is shown that as $D\to+\infty$,

$$\Delta\to-(16/15)(2/\pi)^{\frac{1}{2}}D^{\frac{5}{2}}. \quad \text{(III.21)}$$

Thus

$$\Delta\to-2^{-\frac{1}{2}}(15\pi^3)^{-1}\mu^{\frac{5}{2}}\lambda^5. \quad \text{(III.22)}$$

(III.17), (III.20), and (III.22) lead to the following expression for the pressure p at $T=0$:

$$(p)_{T=0}=(16\pi a)^{-1}\mu^2-8^{\frac{1}{2}}(15\pi^2)^{-1}\mu^{\frac{5}{2}}+\cdots. \quad \text{(III.23)}$$

As remarked before, this expression for the pressure is calculated for a Boltzmann system, but is valid also for a Bose system.

[2] T. D. Lee and C. N. Yang, Phys. Rev. **105**, 119 (1957).
[3] K. Huang and C. N. Yang, Phys. Rev. **105**, 767 (1957). See also C. DeDominicis and P. C. Martin, Phys. Rev. **105**, 1417 (1957).

The particle density ρ and the energy density are easily obtained from (III.23):

$$(\rho)_{T=0} = \frac{d}{d\mu}(p)_{T=0} = (8\pi a)^{-1}\mu - 2^{\frac{1}{2}}(3\pi^2)^{-1}\mu^{\frac{3}{2}} + \cdots, \quad \text{(III.24)}$$

$$(E/\Omega)_{T=0} = \left[\mu\frac{d}{d\mu} - 1\right](p)_{T=0} = (16\pi a)^{-1}\mu^2 - 2^{\frac{1}{2}}(5\pi^2)^{-1}\mu^{\frac{5}{2}} + \cdots. \quad \text{(III.25)}$$

Eliminating μ one obtains the ground-state energy per particle:

$$(E/N)_{T=0} = 4\pi a\rho[1 + 128(\rho a^3)^{\frac{1}{2}}(15\pi^{\frac{1}{2}})^{-1} + \cdots]. \quad \text{(III.26)}$$

The result (III.26) was quoted previously in a short summary.[2] Stimulated by this result, the authors together with K. Huang had investigated the possibility of obtaining the ground-state energy by the pseudopotential method. It turned out that this is indeed possible. A description of these considerations has already been published.[4]

3. CALCULATION OF Γ

To evaluate γ_l is to evaluate b_l to the dominant order (i.e., lowest order) of a/λ. Now b_l is an integral of U_l which in turn, as shown in paper I, is expressible as a sum of integrals of powers of the binary kernel B, starting with the power B^{l-1}. The diagrams that correspond to integrals of B^{l-1} will be called lowest order diagrams, those that correspond to integrals of B^l, next-to-lowest order diagrams. We expand B according to powers of a as in (I.71): $B = B_1 + B_2 + \cdots$ where B_1 is of the order a, B_2 of the order a^2, etc. To the lowest order in a/λ one need only include lowest order diagrams, and replace B by B_1 in them. One thus obtains a term for b_l proportional to a^{l-1}, the coefficient of which, by (III.10) is $\lambda^{-3}\gamma_l(\lambda)^{-l+1}$. For the next order terms there are contributions from

(i) next-to-lowest order diagrams, in which one replaces B^l by $B_1{}^l$, (III.27)

and

(ii) lowest-order diagrams, in which one replaces one of the B's in B^{l-1} by B_2 and the rest by B_1. (III.28)

These contributions are considered in the next section in the calculation of δ_l.

The procedure described above which involves expanding B into powers of a is not[5] one that can be extended in a straightforward manner to all powers of a. In fact, it can be seen that in the next order beyond the terms explicitly written down in (III.10), complications will already be encountered. The origin of these complications lies in the fact that in coordinate space, for fixed $\mathbf{r}_1, \mathbf{r}_2, \cdots \mathbf{r}_1', \mathbf{r}_2' \cdots$, the matrix element

$$\langle \mathbf{r}_1', \mathbf{r}_2', \cdots | U_l | \mathbf{r}_1, \mathbf{r}_2 \cdots \rangle$$

can be expanded in powers of a, starting with the power a^{l-1}, but the expansion does not apply to regions in which, say, $|\mathbf{r}_1 - \mathbf{r}_2| \sim a$ which contribute terms of order $a^3 a^{l-2} = a^{l+1}$ to the coefficients b_l. The calculation in Appendix A, paper II, illustrates this point for the case of b_2.

We now concentrate on the lowest order diagrams and replace B by B_1. We use the momentum representation. As an example, let us first consider b_3, and take the first diagram for U_3 in Fig. 5, paper I. Conservation of momentum forces $\mathbf{k}_a = \mathbf{k}_{1'}$, $\mathbf{k}_c = \mathbf{k}_3$ in this diagram. The contribution to U_3 (to the order a^2) from this diagram is, according to the rules in paper I,

$$\int_0^\beta d\beta' \int_0^{\beta'} d\beta''(a\pi^{-2})^2 \int d^3k_b \exp[-(\beta-\beta'')\mathbf{k}_{1'}{}^2 - (\beta-\beta')\mathbf{k}_{2'}{}^2 - (\beta-\beta')\mathbf{k}_{3'}{}^2]\delta^3(\mathbf{k}_{2'} + \mathbf{k}_{3'} - \mathbf{k}_b - \mathbf{k}_3) \times \exp[-(\beta'-\beta'')\mathbf{k}_b{}^2 - (\beta'-\beta'')\mathbf{k}_3{}^2] \times \delta^3(\mathbf{k}_{1'} + \mathbf{k}_b - \mathbf{k}_1 - \mathbf{k}_2) \times \exp[-\beta''\mathbf{k}_1{}^2 - \beta''\mathbf{k}_2{}^2 - \beta''\mathbf{k}_3{}^2]. \quad \text{(III.29)}$$

The δ function can be used to evaluate the d^3k_b integration. One thus obtains, by (I.54), the following contribution to $\langle \mathbf{k}_{1'}, \mathbf{k}_{2'}, \mathbf{k}_{3'} | u_3 | \mathbf{k}_1, \mathbf{k}_2, \mathbf{k}_3 \rangle$:

$$(a\pi^{-2})^2 \int_0^\beta d\beta' \int_0^{\beta'} d\beta'' \exp[-(\beta-\beta'')\mathbf{k}_{1'}{}^2 - \beta''\mathbf{k}_1{}^2 - (\beta-\beta')\mathbf{k}_{2'}{}^2 - (\beta'-\beta'')\mathbf{k}_b{}^2 - \beta''\mathbf{k}_2{}^2 - (\beta-\beta')\mathbf{k}_{3'}{}^2 - \beta'\mathbf{k}_3{}^2], \quad \text{(III.30)}$$

where $\mathbf{k}_b = \mathbf{k}_1 + \mathbf{k}_2 - \mathbf{k}_{1'}$. To obtain the contribution to b_3 one puts $\mathbf{k}_{i'} = \mathbf{k}_i$, as explicitly shown in (I.55). Therefore $\mathbf{k}_b = \mathbf{k}_2$, and the exponential factor in (III.30) becomes greatly simplified:

$$\exp[-\beta\mathbf{k}_1{}^2 - \beta\mathbf{k}_2{}^2 - \beta\mathbf{k}_3{}^2],$$

which is independent of β' and β''. The contribution to b_3 is thus

$$(3!\,8\pi^3)^{-1}(a\pi^{-2})^2 \int \exp(-\beta\mathbf{k}_1{}^2 - \beta\mathbf{k}_2{}^2 - \beta\mathbf{k}_3{}^2) \times d^3k_1 d^3k_2 d^3k_3 \int_0^\beta d\beta' \int_0^{\beta'} d\beta'' = (3!\,8\pi^3)^{-1}(a\pi^{-2})^2(\pi/\beta)^{9/2}\tfrac{1}{2}\beta^2. \quad \text{(III.31)}$$

The considerations above hold essentially unchanged for higher values of l. One arrives at the following

[4] Lee, Huang, and Yang, Phys. Rev. **106**, 1135 (1957).

[5] The authors are indebted to Dr. T. T. Wu who first raised this question.

contribution to b_l from *each* lowest order diagram:

$$(l!\,8\pi^3)^{-1}(-a\pi^{-2})^{l-1}(\pi/\beta)^{3l/2}\beta^{l-1}/(l-1)!. \quad \text{(III.32)}$$

Defining A_l to be the number of lowest order diagrams, one obtains

$$b_l=\lambda^{-3}(l!)^{-1}[(l-1)!]^{-1}(-2a/\lambda)^{l-1}A_l+0(a^l), \quad (l\geqq 2). \quad \text{(III.33)}$$

Thus,

$$\gamma_l=(l!)^{-1}[(l-1)!]^{-1}(-2)^{l-1}A_l. \quad \text{(III.34)}$$

We define $A_1=1$, so that this equation is also valid for $l=1$.

As will be explained in Fig. 4, the number A_l is the number of "tree skeletons." The mathematical problem of calculating A_l by generating functions will be solved in Appendix C. Equation (III.99) there together with (III.11) gives

$$\Gamma(x)=\tfrac{1}{2}D+\tfrac{1}{4}D^2,$$

which was used before in (III.12).

4. CALCULATION OF Δ

As already discussed in the last section, the contributions to δ_l come from (III.27) and (III.28). We shall

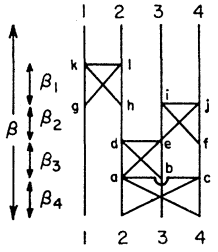

FIG. 1. Example of a next-to-lowest order diagram for $l=4$. The intervals β_1, β_2, $\cdots\beta_l$ are always labeled from the top down.

discuss (III.27) first. Each next-to-lowest order diagram contains l B's. These B's carry with them factors of δ functions showing the conservation of momentum. To see the effect of these δ functions we draw a skeleton (Fig. 2) for each next-to-lowest order diagram (Fig. 1). As Fig. 2 shows, each skeleton consists of l numbered points connected by l lines, μ of which form a simple loop, the rest not forming loops. The lines are labeled by $\beta_1, \beta_2, \cdots\beta_l$. Different labelings give rise to different skeletons. For the case of $\mu=2$, one line is doubled, and must be labeled twice, by two intervals β_m, β_n. Notice that $|m-n|\neq 1$ in order that B does not operate between the same two particles in immediate succession. See Fig. 3. With this provision in the definition of a skeleton, there is a one-to-one correspondence between a next-to-lowest order diagram and a skeleton. Some additional examples of skeletons are shown in Fig. 3. Now each B between i and j produces a transfer of momentum between particles i and j. For diagonal elements of U_l, the momenta of all particles after the l transfers of momenta must be the same as their original values. Hence the momentum *transfer* $\mathbf{p}$ must be the same for all B's within the loop,

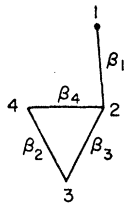

FIG. 2. Skeleton that corresponds to Fig. 1. Each line between i and j represents a B operator between the particles i and j. The order of the operators B are specified by the β_α's that label the lines. Each next-to-lowest order diagram corresponds uniquely to one skeleton with l lines, μ of which forms a simple loop while the rest do not form loops. In this skeleton $\mu=3$. The case of $\mu=2$ is special and is discussed in detail in the text. See also Fig. 3.

and 0 for the other lines. As an example, take the skeleton shown in Fig. 2. The momentum transfer from 4 to 2 during β_4 is the same as that from 2 to 3 during β_3 and also the same as that from 3 to 4 during β_2 and will be denoted by $\mathbf{p}$. In Fig. 1, this means that the momenta of the points $a, b, \cdots l$ are given by

$$\mathbf{k}_a=\mathbf{k}_2+\mathbf{p}, \quad \mathbf{k}_b=\mathbf{k}_3, \quad \mathbf{k}_c=\mathbf{k}_4-\mathbf{p}, \quad \mathbf{k}_d=\mathbf{k}_2,$$
$$\mathbf{k}_e=\mathbf{k}_3+\mathbf{p}, \quad \mathbf{k}_f=\mathbf{k}_4-\mathbf{p}, \quad \mathbf{k}_g=\mathbf{k}_1, \quad \mathbf{k}_h=\mathbf{k}_2,$$
$$\mathbf{k}_i=\mathbf{k}_3, \quad \mathbf{k}_j=\mathbf{k}_4, \quad \mathbf{k}_k=\mathbf{k}_1, \quad \mathbf{k}_l=\mathbf{k}_2. \quad \text{(III.35)}$$

The above reasoning shows that for a particle i (e.g., $i=1$ in Fig. 1) not in the loop, no momentum transfers ever occur so that the momentum is always $\mathbf{k}_i$. For a particle i in the loop, as one proceeds up vertically in the next-to-lowest order diagram, the particle may first receive a momentum $\mathbf{p}$ and then lose it (e.g., $i=2$ or $i=3$ in Fig. 1), or vice versa, (e.g., $i=4$ in Fig. 1). In the former case, its momentum starts out as $\mathbf{k}_i$, becomes $\mathbf{k}_i+\mathbf{p}$, and then changes back to $\mathbf{k}_i$. In the latter case, its momentum starts out as $\mathbf{k}_i$, becomes $\mathbf{k}_i-\mathbf{p}$, and then changes back to $\mathbf{k}_i$.

Now by (I.71), B_1 contains an exponential factor and a δ function. To calculate the contribution to b_l due to a next-to-lowest order diagram, one uses (I.54) and (I.55). The δ functions can be used to reduce the $\mathbf{k}$ integration for intermediate $\mathbf{k}$'s in the manner discussed above. One obtains thus a contribution to b_l equal to

$$b_l'=(l!\,8\pi^3)^{-1}(-a/\pi^2)^l\int d\beta_1\cdots d\beta_l$$
$$\times\int d^3p\int d^3k_1 d^3k_2\cdots d^3k_l$$
$$\times\exp[-\sum_1^l\beta_\alpha E_\alpha-E_0(\beta-\sum_1^l\beta_\alpha)], \quad \text{(III.36)}$$

where $E_0=k_1^2+k_2^2+\cdots+k_l^2$, and $E_\alpha=$ the energy in the diagram at the horizontal level corresponding to the bottom on the β_α interval. The β integration extends over positive values of β_α for which $\sum_1^l\beta_\alpha\leqq\beta$. For the example in Fig. 1,

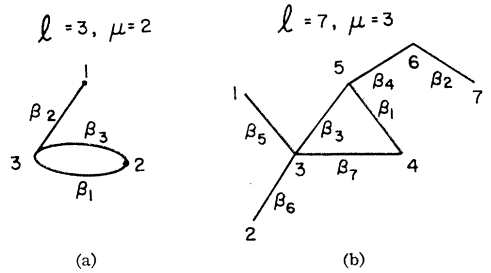

(a) (b)

FIG. 3. Further examples of skeletons. Notice that if the labels β_1 and β_2 are interchanged in skeleton 3(a), the result is not a skeleton because the B operator between particles 2 and 3 would in that case act in the intervals β_2, β_3. No next-to-lowest order diagram corresponds to such a case.

$$E_1=\mathbf{k}_g^2+\mathbf{k}_h^2+\mathbf{k}_i^2+\mathbf{k}_j^2=\mathbf{k}_1^2+\mathbf{k}_2^2+\mathbf{k}_3^2+\mathbf{k}_4^2,$$
$$E_2=\mathbf{k}_1^2+\mathbf{k}_d^2+\mathbf{k}_e^2+\mathbf{k}_f^2=\mathbf{k}_1^2+\mathbf{k}_2^2+(\mathbf{k}_3+\mathbf{p})^2+(\mathbf{k}_4-\mathbf{p})^2, \quad \text{(III.37)}$$
$$E_3=\mathbf{k}_1^2+\mathbf{k}_a^2+\mathbf{k}_b^2+\mathbf{k}_c^2=\mathbf{k}_1^2+(\mathbf{k}_2+\mathbf{p})^2+\mathbf{k}_3^2+(\mathbf{k}_4-\mathbf{p})^2,$$
$$E_4=E_0.$$

The exponent of the integrand in (III.36) is a sum of terms $\mathbf{k}_i^2$, $(\mathbf{k}_i\pm\mathbf{p})^2$. The d^3k_i integration is thus a Gaussian integral:

$$\int d^3k_i \exp[-s_i(\mathbf{k}_i\pm\mathbf{p})^2-(\beta-s_i)\mathbf{k}_i^2] = (2\pi/\lambda)^3 \exp[-\beta^{-1}p^2 s_i(\beta-s_i)], \quad \text{(III.38)}$$

where $s_i=\sum\beta_\alpha$ over all α for which E_α contains $(\mathbf{k}_i\pm\mathbf{p})^2$. For example, from (III.37), one sees that for the diagram of Fig. 1,

$$s_1=0, \quad s_2=\beta_3, \quad s_3=\beta_2, \quad s_4=\beta_2+\beta_3. \quad \text{(III.39)}$$

A simple rule for writing down s_i will be given below. Combining (III.38) with (III.36), one obtains

$$b_l'=(l!\,8\pi^3)^{-1}(-8\pi a/\lambda^3)^l\int_{\Sigma\beta_\alpha\leqq\beta} d\beta_1\cdots d\beta_l \times\int d^3p \exp[-\beta^{-1}p^2\sum s_i(\beta-s_i)]. \quad \text{(III.40)}$$

Now let us introduce the variables

$$\xi_1=\beta_1+\beta_2+\cdots+\beta_l, \quad \xi_2=\beta_2+\beta_3+\cdots+\beta_l, \cdots, \quad \xi_l=\beta_l. \quad \text{(III.41)}$$

One finds

$$b_l'=(l!\,8\pi^3)^{-1}(-8\pi a/\lambda^3)^l\int_{\beta\geqq\xi_1\geqq\xi_2\cdots\geqq\xi_l\geqq0} d\xi_1\cdots d\xi_l \times\int d^3p \exp[-\beta^{-1}p^2\sum s_i(\beta-s_i)]. \quad \text{(III.42)}$$

We also change the labeling of the lines in the skeleton $\beta_i\to\xi_i$. The *important observation* is that s_i can be read off the relabeled skeleton according to the following rule:

$s_i=0$ for i not in the loop; otherwise

$s_i=|$ difference of the two ξ's labeling the two lines in the loop touching the vertex $i|$. (III.43)

(III.43) gives, for each relabeled skeleton, s_i as explicit functions of ξ_α.

We now take an "unlabeled skeleton" with $\mu\geqq3$ and consider all the $l!$ ways of labeling it. Each gives rise to a skeleton and contributes a term b_l'. These $l!$ contributions are in general different. The sum of them is, by (III.42) and (III.43),

$$\Theta_{l,\mu}=(l!\,8\pi^3)^{-1}(-8\pi a/\lambda^3)^l\int_{\beta\geqq\xi_\alpha\geqq0} d\xi_1\cdots d\xi_l\int d^3p \times\exp[-\beta^{-1}p^2\sum s_i(\beta-s_i)], \quad \text{(III.44)}$$

where s_i is given by (III.43) for any particular way L of labeling. [Notice that the region of ξ integration in (III.44) is much enlarged compared with that of (III.42).] We choose L so that the lines in the loop are successively labeled ξ_1, ξ_2, $\cdots\xi_\mu$. The integrand in (III.44) is then independent of $\xi_{\mu+1}$, $\xi_{\mu+2}$, $\cdots\xi_l$. Thus

$$\Theta_{l,\mu}=(l!\,8\pi^3)^{-1}(-8\pi a/\lambda^3)^l\beta^{l-\mu}\int_{\beta\geqq\xi_\alpha\geqq0} d\xi_1\cdots d\xi_\mu \times\int d^3p \exp\{-\beta^{-1}p^2[(\xi_{12}\beta-\xi_{12}^2)+(\xi_{23}\beta-\xi_{23}^2)+\cdots+(\xi_{\mu1}\beta-\xi_{\mu1}^2)], \quad \text{(III.45)}$$

where

$$\xi_{12}=|\xi_1-\xi_2|, \quad \text{etc.} \quad \text{(III.46)}$$

Introducing the variables $t_\alpha=\xi_\alpha\beta^{-1}$, $q=p^2\beta$, one obtains

$$\Theta_{l,\mu}=\lambda^{-3}(l!)^{-1}(-2a/\lambda)^l c_\mu, \quad \text{(III.47)}$$

where c_μ was defined before in (III.15).

We have shown above that each "unlabeled skeleton" (or rather, all the skeletons with $\mu\geqq3$ corresponding to one unlabeled skeleton) contributes to b_l the expression $\Theta_{l,\mu}$ given by (III.47). The total contribution from all unlabeled skeletons for given l and μ ($l\geqq\mu\geqq3$) is thus

$$\lambda^{-3}(l!)^{-1}(-2a/\lambda)^l c_\mu\Xi(\mu,l), \quad \text{(III.48)}$$

where $\Xi(\mu,l)$ is the number of unlabeled skeletons with l numbered points, and l (unlabeled undirected) lines, μ of which form a simple loop while the rest do not form loops. Comparing (III.48) with (III.10) we obtain the contribution to δ_l from all skeletons with $\mu\geqq3$:

$$\sum_{\mu=3}^{l}(l!)^{-1}(-2)^l c_\mu\Xi(\mu,l). \quad \text{(III.49)}$$

We must now add to this the contribution from skeletons with $\mu=2$. For this case (III.42) and (III.43) still hold for each skeleton, but not all labelings of an unlabeled skeleton are allowed, as discussed in the first paragraph of this section. One therefore obtains (III.44) taken at $\mu=2$, minus the contribution that corresponds to consecutive labeling of the two lines in

the loop. The result must be divided by two because, e.g., in Fig. 3(a), switching the labels β_1 and β_3 do not generate new skeletons. Thus, each "unlabeled skeleton" with $\mu=2$ gives the following contribution to b_l:

$$\Theta_{l,2}=(l!\,8\pi^3)^{-1}(-8\pi a/\lambda^3)^l\frac{1}{2}\int_{\beta\geqq\xi_\alpha\geqq 0}d\xi_1\cdots d\xi_l \times\int d^3p[-2\beta^{-1}p^2\xi_{12}(\beta-\xi_{12})] - (l!\,8\pi^3)^{-1}(-8\pi a/\lambda^3)^l\frac{1}{2}\int_{\mathfrak{R}}d\xi_1\cdots d\xi_l \times\int d^3p[-2\beta^{-1}p^2\xi_{12}(\beta-\xi_{12})], \quad \text{(III.50)}$$

where ξ_{12} is defined in (III.47) and $\mathfrak{R}$ is a region in ξ space corresponding to $\beta\geqq\xi_\alpha\geqq 0$, but with no ξ_α falling in the interval between ξ_1 and ξ_2. The p integration in (III.50) can be carried out. Changing variables from ξ to t, $\xi_\alpha=\beta t_\alpha$, one obtains

$$\Theta_{l,2}=\lambda^{-3}(l!)^{-1}(-2a/\lambda)^l\phi_l, \quad \text{(III.51)}$$

where

$$\phi_l=\frac{1}{2}\int_0^1\int_0^1[2t_{12}(1-t_{12})]^{-\frac{3}{2}}\times[1-(1-t_{12})^{l-2}]dt_1dt_2 =\int_0^1 t[2t(1-t)]^{-\frac{3}{2}}[1-t^{l-2}]dt, \quad (l\geqq 2). \quad \text{(III.52)}$$

We thus obtain

$$\delta_l=(l!)^{-1}(-2)^l\phi_l\Xi(2,l)+\sum_{\mu=3}^{l}(l!)^{-1}(-2)^lc_\mu\Xi(\mu,l) +\text{contribution from (III.28).} \quad \text{(III.53)}$$

We shall now explicitly calculate the contribution from (III.28) to δ_l. We consider a lowest order diagram in which one specific B is replaced by B_2, the other B's by B_1. We call this a *marked diagram* [the B_2 being marked]. For every marked diagram, by the same reasoning that led to (III.31), one concludes that in the diagram all the intermediate momenta of particle i are the same as the original value $\mathbf{k}_i$. The contribution to b_l from the diagram is, by (I.54) and (I.55), given by an integral over $d^3k_1\cdots d^3k_l$, the integrand itself being given by an integral over $d\beta_1d\beta_2\cdots d\beta_{l-1}$. Using the explicit forms (I.71) for B_1 and B_2, one sees that all d^3k integrations can be immediately carried out except for the two involved in B_2. Also the $d\beta$ integrations can be carried out except for the one involved in B_2. One arrives thus at the following contribution to b_l:

$$(l!\,8\pi^3)^{-1}(-a\pi^{-2})^{l-2}\pi^{-(\frac{5}{2})}a^2(\pi/\beta)^{3(l-2)/2} \times\int_0^\beta d\beta_1(\beta-\beta_1)^{l-2}[(l-2)!]^{-1}\int\int d^3k_1d^3k_2 \times[\exp(-\beta k_1^2-\beta k_2^2)][2kM((2\beta_1)^{\frac{1}{2}}k) -(2\beta_1)^{-\frac{1}{2}}\exp(2\beta_1k^2)], \quad \text{(III.54)}$$

where $k=\frac{1}{2}|\mathbf{k}_1-\mathbf{k}_2|$ and M was defined in (I.68). Different ways of marking the same diagram lead to the same contribution (III.54). We should therefore multiply (III.54) by $(l-1)$ which is the number of ways a diagram can be marked. We should also multiply by $A_l=$ the number of lowest-order diagrams, a number already introduced in Sec. 3. The contribution of (III.28) to b_l is thus

$$(l-1)A_l\times\text{(III.54)}. \quad \text{(III.55)}$$

The integral in (III.54) can be evaluated by first transforming $\mathbf{k}_1$ and $\mathbf{k}_2$ into the center-of-mass momentum $\mathbf{K}$ and relative momentum $\mathbf{k}$:

$$\mathbf{K}=\mathbf{k}_1+\mathbf{k}_2, \quad \mathbf{k}=\tfrac{1}{2}(\mathbf{k}_1-\mathbf{k}_2).$$

The $\mathbf{K}$ integration is then performed and one is left with the following k integration:

$$\int_0^\infty k^2[\exp(-2\beta k^2)][2kM((2\beta_1)^{\frac{1}{2}}k) -(2\beta_1)^{-\frac{1}{2}}\exp(2\beta_1k^2)]dk,$$

which one evaluates by writing

$$M((2\beta_1)^{\frac{1}{2}}k)=(2\beta_1)^{\frac{1}{2}}\int_0^k\exp(2\beta_1p^2)dp,$$

and then switching the p and k integrations. One is left after these integrations with only the β_1 integration. After the transformation $\beta_1=\beta t$ one arrives at

$$\text{(III.54)}=-[\sqrt{2}\lambda^3l!(l-2)!]^{-1}(-2a/\lambda)^l\chi_l,$$

where

$$\chi_l=\int_0^1 t^{l-2}(2t-1)[t(1-t)]^{-\frac{1}{2}}dt. \quad \text{(III.56)}$$

Substituting this into (III.55) one obtains the following contribution to δ_l from (III.28):

$$-(l-1)A_l[\sqrt{2}l!(l-2)!]^{-1}(-2)^l\chi_l, \quad \text{(III.57)}$$

which, together with (III.53) gives the complete explicit expression for δ_l.

We shall now show that (III.57) exactly cancels the first term on the right-hand side of (III.53) so that

$$\delta_l=\sum_{\mu=3}^{l}(l!)^{-1}(-2)^lc_\mu\Xi(\mu,l). \quad \text{(III.58)}$$

To show this cancellation we compare the definitions of $\Xi(2,l)$ and A_l. Their differences are: (i) For Ξ one

considers unlabeled skeletons, while for A_l one considers labeled ones. (ii) For skeletons counted in $\Xi(2,l)$ one of the lines is doubled [i.e., one may think of $(l-1)$ lines with one of them drawn twice over]. These two differences give rise to factors $(l-1)!$ and $(l-1)$, respectively. Thus

$$\frac{\Xi(2,l)}{l-1}=\frac{A_l}{(l-1)!}. \tag{III.59}$$

The integrals in (III.52) and (III.56) can be evaluated by putting $t=\sin^2\theta$. One obtains thus

$$\phi_l=\sqrt{2}^{-1}(l-1)\chi_l. \tag{III.60}$$

Using (III.59) and (III.60) one easily proves the cancellation, and therefore (III.58).

The cancellation in terms of diagrams means that next-to-lowest order diagrams with two B_1's interacting between the same two particles i and j are exactly cancelled (to the order considered) by contributions from the lowest-order diagrams. This is a simple result which probably has a simple interpretation and a derivation more deeply rooted than the above brute-force explicit evaluation.

To evaluate the generating function Δ defined in (III.11) from the δ_l of (III.58), we use Eq. (III.105) derived in Appendix D. The result is Eq. (III.14) used above in Sec. 2.

APPENDIX A

We shall find the asymptotic limits of $g_{\frac{5}{2}}$, $g_{\frac{3}{2}}$, $g_{\frac{1}{2}}$, and F for arguments $-z\to-\infty$. Now

$$-g_{\frac{3}{2}}(-z)=\pi^{-\frac{3}{2}}\int_0^\infty \frac{z\exp(-k^2)}{1+z\exp(-k^2)}d^3k$$
$$=\pi^{-\frac{3}{2}}\int_0^\infty \frac{z}{z+\exp(k^2)}d^3k. \tag{III.61}$$

For large values of z, the integrand is ~1 for $k\ll(\ln z)^{\frac{1}{2}}$ and is ~0 for $k\gg(\ln z)^{\frac{1}{2}}$. The range of values of k in which the integrand is different from its limiting value is $\sim(\ln z)^{-\frac{1}{2}}$. These considerations lead easily to the following asymptotic limit:

$$-g_{\frac{3}{2}}(-z)=4(9\pi)^{-\frac{1}{2}}(\ln z)^{\frac{3}{2}}+6^{-1}\pi^{\frac{3}{2}}(\ln z)^{-\frac{1}{2}}$$
$$+O([\ln z]^{-\frac{5}{2}}). \tag{III.62}$$

By differentiation one obtains

$$-g_{\frac{1}{2}}(-z)=2\pi^{-\frac{1}{2}}(\ln z)^{\frac{1}{2}}-(12)^{-1}\pi^{\frac{3}{2}}(\ln z)^{-\frac{3}{2}}$$
$$+O([\ln z]^{-7/2}). \tag{III.63}$$

And by integration one obtains

$$-g_{\frac{5}{2}}(-z)=8(15\pi^{\frac{1}{2}})^{-1}(\ln z)^{\frac{5}{2}}+3^{-1}\pi^{\frac{3}{2}}(\ln z)^{\frac{1}{2}}+O(1). \tag{III.64}$$

To find the asymptotic behavior of F for arguments $-z\to-\infty$ we first observe that the coefficients in the series (III.3) can be expressed as integrals:

$$(rst)^{-\frac{1}{2}}(r+s)^{-1}(r+t)^{-1}=8\pi^{-\frac{3}{2}}\int_0^\infty \exp[-X^2r-Y^2s$$
$$-Z^2t-\xi(r+s)-\eta(r+t)]dXdYdZd\xi d\eta.$$

Thus

$$-F(-z)=8\pi^{-\frac{3}{2}}\int_0^\infty \frac{z}{z+\exp(X^2+\xi+\eta)}$$
$$\times\frac{z}{z+\exp(Y^2+\xi)}\frac{z}{z+\exp(Z^2+\eta)}$$
$$\times dXdYdZd\xi d\eta. \tag{III.65}$$

The asymptotic form of this integral can be obtained in the same way as that for the integral in (III.61): For large z, the integrand is ~1 in the region R:

$$\begin{aligned} X^2+\xi+\eta&\leqq\ln z,\\ Y^2+\xi&\leqq\ln z,\\ Z^2+\eta&\leqq\ln z,\end{aligned} \tag{III.66}$$

and is ~0 outside. The dominant term is therefore given by

$$-F(-z)\to 8\pi^{-\frac{3}{2}}\int_R dXdYdZd\xi d\eta.$$

This integral can be evaluated in a straightforward way, yielding

$$-F(-z)=16(11-2\ln 2)(105)^{-1}\pi^{-\frac{3}{2}}(\ln z)^{7/2}$$
$$+O([\ln z]^{\frac{3}{2}}). \tag{III.67}$$

APPENDIX B

To study the limiting form of $\Delta(x)$ [defined in (III.14)–(III.16)] for large x, we first notice that D was defined by

$$De^D=x,$$

so that as $x\to+\infty$, $D\to+\infty$. Defining a Hermitian operator

$$\langle t'|\mathfrak{B}|t\rangle=\exp[-q|t-t'|+q(t-t')^2], \tag{III.68}$$

where t and t' range from 0 to 1, one can write (III.15) as

$$c_\mu=2\pi^{-\frac{1}{2}}\int_0^\infty q^{\frac{1}{2}}\ \text{trace}\ \mathfrak{B}^\mu dq. \tag{III.69}$$

Substitute this into (III.14). One obtains

$$\Delta=-\pi^{-\frac{1}{2}}\int_0^\infty q^{\frac{1}{2}}dq\psi, \tag{III.70}$$

where

$$\psi=\text{trace}[\ln(1+\mathfrak{B}D)-\mathfrak{B}D+\tfrac{1}{2}D^2\mathfrak{B}^2]. \tag{III.71}$$

Clearly

$$\psi=\textstyle\sum_m[\ln(1+D\lambda_m)-D\lambda_m+\frac{1}{2}D^2\lambda_m{}^2], \tag{III.72}$$

where λ_m are the eigenvalues of $\mathfrak{B}$. Since $\mathfrak{B}$ by definition (III.68) is a cyclic matrix, the eigenvectors are $e^{2\pi imt}$ ($m=\pm$integer or 0), and the eigenvalues

$$\lambda_m=\int_0^1 dt[\cos 2\pi mt]\exp[-qt(1-t)]. \quad \text{(III.73)}$$

We first study the convergence of the sums and integrals in the definitions of ψ and in (III.70). It is clear that

$$\sum_m \lambda_m=\operatorname{trace}\mathfrak{B}=1, \quad \text{(III.74)}$$

$$\sum_m \lambda_m{}^2=\operatorname{trace}\mathfrak{B}^2\leqq 2/q. \quad \text{(III.75)}$$

Similarly,

$$\sum_m \lambda_m{}^3=\operatorname{trace}\mathfrak{B}^3\leqq 16/q^2. \quad \text{(III.76)}$$

Furthermore by (III.73), it is easily seen that

$$\begin{aligned}&\lambda_m>0 \quad \text{for} \quad q>0,\\ &\lambda_m=\delta_{m0} \quad \text{for} \quad q=0.\end{aligned} \quad \text{(III.77)}$$

Using these properties and the fact that for $x>0$,

$$0\leqq \ln(1+x)-x+\tfrac{1}{2}x^2\leqq \tfrac{1}{3}x^3,$$

it is easy to show that for $D>0$,

$$0\leqq\psi\leqq\tfrac{1}{3}D^3\sum_m\lambda_m{}^3\leqq 16D^3/(3q^2). \quad \text{(III.78)}$$

Thus Δ as defined by (III.70) is convergent at large q. Furthermore since the λ_m's are all positive and $\leqq 1$, $\sum\lambda_m{}^3\leqq\sum\lambda_m=1$. Hence

$$\psi\leqq\tfrac{1}{3}D^3. \quad \text{(III.79)}$$

Hence Δ is also convergent at small q. In fact, by (III.78) and (III.79) one easily proves that for all $D>0$,

$$0\leqq-\Delta\pi^{\frac{1}{2}}<KD^3,$$

where K is some number.

To study the value of Δ for large D we prove successively the following theorems:

Theorem 1.—

$$\lambda_m/2q[q^2+4\pi^2m^2]^{-1}\to 1, \quad \text{as} \quad q\to\infty.$$

Furthermore the approach to the limit is uniform with respect to m.

Proof.—We take (III.73) and write it as

$$\lambda_m=\int_0^{\frac{1}{2}}[\exp(-qt+qt^2+i2\pi mt)+\text{complex conj.}]dt,$$

in which for large q, only the region, where t is small, contributes. Writing

$$\exp(-qt+i2\pi mt)dt=(2\pi mi-q)^{-1}d[\exp(-qt+i2\pi mt)],$$

one can integrate by parts. It is then easy to prove the theorem.

Theorem 2.—Defining

$$\Lambda_m=2q(q^2+4\pi^2m^2)^{-1}, \quad \text{(III.80)}$$

one has

$$\lim_{q\to\infty}\frac{\sum_m[\lambda_m(1+D\lambda_m)^{-1}-\lambda_m+D\lambda_m{}^2]}{\sum_m[\Lambda_m(1+D\Lambda_m)^{-1}-\Lambda_m+D\Lambda_m{}^2]}=1,$$

uniformly with respect to D ($D\geqq 0$).

Proof.—

$$\lambda_m(1+D\lambda_m)^{-1}-\lambda_m+D\lambda_m{}^2=D^2\lambda_m{}^3(1+D\lambda_m)^{-1}.$$

One can then prove the theorem with this formula.

Theorem 3.—

$$\lim_{q\to\infty}\frac{\sum_m[\Lambda_m(1+D\Lambda_m)^{-1}-\Lambda_m+D\Lambda_m{}^2]}{1+(2D/q)^{-\frac{1}{2}}-1+(D/q)}=1, \quad \text{(III.81)}$$

uniformly with respect to D ($D\geqq 0$).

Proof.—It is straightforward to calculate

$$\sum_m\Lambda_m(1+D\Lambda_m)^{-1},$$

using (III.80) and the formula

$$\sum_{m=-\infty}^{\infty}(m^2+A^2)^{-1}=\pi A^{-1}\coth\pi A. \quad \text{(III.82)}$$

Similarly one can calculate $\sum\Lambda_m$ and $\sum\Lambda_m{}^2$ using the derivative of (III.82) with respect to A. One obtains thus

$$\sum_m[\Lambda_m(1+D\Lambda_m)^{-1}-\Lambda_m+D\Lambda_m{}^2]=\xi(q,x)-\xi(q,0)-x\frac{\partial\xi}{\partial x}(q,0), \quad \text{(III.83)}$$

where $x=D/q$ and

$$\xi(q,x)=(1+2x)^{-\frac{1}{2}}\coth[\tfrac{1}{2}q(1+2x)^{\frac{1}{2}}]. \quad \text{(III.84)}$$

To prove (III.81) is therefore equivalent to proving

$$\lim_{q\to\infty}\frac{\xi(q,x)-\xi(q,0)-x(\partial\xi/\partial x)(q,0)}{\xi(\infty,x)-\xi(\infty,0)-x(\partial\xi/\partial x)(\infty,0)}=1, \quad \text{(III.85)}$$

uniformly with respect to x ($x\geqq 0$). It is trivial to prove (III.85) for any given $x>0$. To prove the uniformity of convergence, however, one must remember that the denominator vanishes at $x=0$. The region near $x=0$ therefore needs special treatment. Such a treatment is however, not difficult to formulate upon using the mean value theorem on both the numerator and denominator of the left side of (III.85).

Theorem 4.—

$$\lim_{q\to\infty}\psi^{-1}[(q^2+2Dq)^{\frac{1}{2}}-q-D+(D^2/2q)]=1, \quad \text{(III.86)}$$

uniformly with respect to D. [$D\geqq 0$. ψ is defined by (III.72).]

Proof.—One uses Theorems 2 and 3 and obtains, for every $Q>0$, a $K_Q>0$ such that for $D\geqq 0$,

$$\begin{aligned}&\sum[\lambda_m(1+D\lambda_m)^{-1}-\lambda_m+D\lambda_m{}^2]\\ &\quad>\{[1+(2D/q)]^{-\frac{1}{2}}-1+(D/q)\}(1-K_Q),\\ &\sum[\lambda_m(1+D\lambda_m)^{-1}-\lambda_m+D\lambda_m{}^2]\\ &\quad<\{[1+(2D/q)]^{-\frac{1}{2}}-1+(D/q)\}(1+K_Q),\end{aligned} \quad \text{(III.87)}$$

for all $q>Q$. Here K_Q depends on Q and $\to 0$ as $Q\to+\infty$. Integrating both sides of (III.87) with respect to D from $D=0$ to $D=D$, one obtains

$$\psi>[(q^2+2Dq)^{\frac{1}{2}}-q-D+(D^2/2q)][1-K_Q],$$
$$\psi<[(q^2+2Dq)^{\frac{1}{2}}-q-D+(D^2/2q)][1+K_Q], \quad \text{(III.88)}$$

which is identical with (III.86). This completes the proof.

We are now in a position to calculate Δ for large D. We break the $\int_0^\infty dq$ into $\int_0^Q dq+\int_Q^\infty dq$. Now

$$0\leqq\int_0^Q q^{\frac{1}{2}}dq\psi\leqq\int_0^Q q^{\frac{1}{2}}dq[\textstyle\sum_m \frac{1}{2}D^2\lambda_m{}^2].$$

Using (III.75) one obtains

$$0\leqq\int_0^Q q^{\frac{1}{2}}dq\psi\leqq 2D^2Q^{\frac{1}{2}}. \quad \text{(III.89)}$$

Using (III.88) one obtains

$$\int_Q^\infty q^{\frac{1}{2}}dq\,\psi>(1-K_Q)\int_Q^\infty q^{\frac{1}{2}}dq[(q^2+2Dq)^{\frac{1}{2}}-q-D+(D^2/2q)],$$
$$\int_Q^\infty q^{\frac{1}{2}}dq\,\psi<(1+K_Q)\int_Q^\infty q^{\frac{1}{2}}qd[(q^2+2Dq)^{\frac{1}{2}}-q-D+(D^2/2q)]. \quad \text{(III.90)}$$

The right-hand side of (III.90) is evaluable explicitly, yielding

$$\int_Q^\infty q^{\frac{1}{2}}dq\,\psi>(1-K_Q)[(4/15)(Q+2D)^{\frac{5}{2}}-\tfrac{2}{3}Q(Q+2D)^{\frac{3}{2}}+\tfrac{2}{5}Q^{\frac{5}{2}}+\tfrac{2}{3}DQ^{\frac{3}{2}}-D^2Q^{\frac{1}{2}}],$$
$$\int_Q^\infty q^{\frac{1}{2}}dq\,\psi<(1+K_Q)[(4/15)(Q+2D)^{\frac{5}{2}}-\tfrac{2}{3}Q(Q+2D)^{\frac{3}{2}}+\tfrac{2}{5}Q^{\frac{5}{2}}+\tfrac{2}{3}DQ^{\frac{3}{2}}-D^2Q^{\frac{1}{2}}]. \quad \text{(III.91)}$$

For $D\gg Q$, the term $(Q+2D)^{\frac{5}{2}}$ dominates, From (III.91) and (III.89) one concludes that, according to (III.70),

$$\Delta\to-\pi^{-\frac{1}{2}}(4/15)(2D)^{\frac{5}{2}} \quad \text{as} \quad D\to+\infty.$$

This is the result (III.21) used in the text.

APPENDIX C

The number A_l first introduced in (III.33) is the number of lowest order diagrams for b_l. Now the lowest order diagrams have a one-to-one correspondence with "tree skeletons" as explained in the caption of Fig. 4. A_l is therefore the number of tree skeletons for l points. One has by direct enumeration

$$A_2=1, \quad A_3=6, \quad A_4=96, \quad \cdots.$$

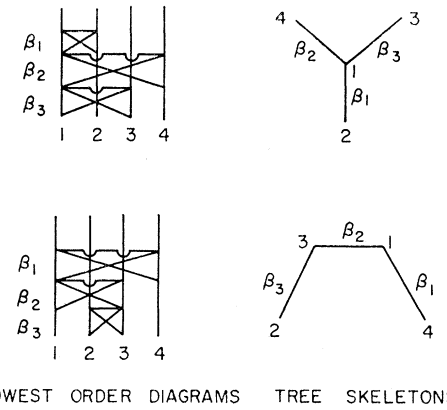

FIG. 4. One-to-one correspondence between lowest-order diagrams and tree skeletons. Each tree skeleton consists of l points $1, 2, \cdots l$ connected by $(l-1)$ lines without loop formation. The lines are labeled by $\beta_1, \cdots \beta_{l-1}$. A line in the tree skeleton between points i and j represents an operator B between i and j in the lowest order diagram, its label β_α represents its vertical duration in the lowest order diagram. The order of the operators B are specified by the labeling β_α's. Different labelings give different tree skeletons.

We define

$$A_l'\equiv A_l[(l-1)!]^{-1}, \quad A_l''=A_l[(l-1)!]^{-2}. \quad \text{(III.92)}$$

A_l' is the number of *unlabeled* tree skeletons (i.e., tree skeletons without the labeling $\beta_1, \cdots \beta_{l-1}$ of the lines). Now each unlabeled tree skeleton can be broken into two disconnected pieces [in $2(l-1)$ ways] by (i) breaking one of the $(l-1)$ lines, and (ii) marking one of the sections of the broken line with a star. An example of such a breaking process is shown in Fig. 5. The A_l' different unlabeled tree skeletons can be broken in this way into a totality of $2(l-1)A_l'$ different graphs of the type of Fig. 5. Now each graph consists of (a) an unlabeled tree skeleton of m points with a broken section of a line attached, and (b) an unlabeled tree skeleton of $(l-m)$ points, with a starred, broken section of a line attached. For each fixed way of partition of the numbers $1, 2, \cdots l$ between the two parts, there are mA_m' possible parts (a) and $(l-m)A_{l-m}'$ possible parts (b). These statements are also correct for $m=1$ if we define

$$A_m'=1.$$

Thus

$$2(l-1)A_l'=\sum_{m=1}^{l-1}(mA_m')[(l-m)A_{l-m}']\times\left[\frac{l!}{m!(l-m)!}\right]. \quad \text{(III.93)}$$

In terms of the A_l'' defined in (III.92), this equation reduces to

$$2(l-1)l^{-1}A_l''=\sum_{m=1}^{l-1}A_m''A_{l-m}''. \quad \text{(III.94)}$$

Multiply both sides by $(-x)^l$ and summing over l,

one obtains

$$-2x(dh/dx)+2h=(xdh/dx)^2, \quad \text{(III.95)}$$

where

$$h(x)=-\sum_{l=1}^{\infty} l^{-1}A_l''(-x)^l. \quad \text{(III.96)}$$

Equation (III.95) can be easily solved, giving

$$x(dh/dx)=D, \quad \text{(III.97)}$$

and

$$h=\tfrac{1}{2}D^2+D, \quad \text{(III.98)}$$

where D was defined in (III.13) as given by

$$De^D=x.$$

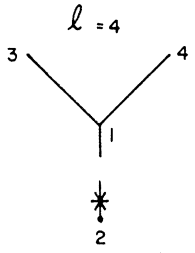

FIG. 5. Example of the breaking of an unlabeled tree skeleton.

Combining (III.92), (III.96), and (III.98), one obtains

$$-\sum_{l=1}^{\infty} l^{-1}[(l-1)!]^{-2}A_l(-x)^l=D+\tfrac{1}{2}D^2. \quad \text{(III.99)}$$

APPENDIX D

We study the properties of $\Xi(\mu,l)$ here for $\mu>2$. [The case for $\mu=2$ was already discussed in (III.59).] We recall that $\Xi(\mu,l)$ was defined immediately after (III.48).

Each unlabeled skeleton with l points 1, 2, $\cdots l$ can be broken at a nonloop line in $(l-\mu)$ ways (see Fig. 6). The two resulting disconnected parts are of the general type of (a) an unlabeled tree skeleton with m points (see Appendix C) and (b) an unlabeled skeleton belonging to the type $\Xi(\mu, l-m)$, each of the two parts having a segment of the broken line attached to it. There are $[m!(l-m)!]^{-1}l!$ ways to partition the points 1, 2, $\cdots l$ to these two pieces. For each partition there are mA_m' possible parts (a) and $(l-m)\Xi(\mu, l-m)$ possible parts (b). Thus

$$(l-\mu)\Xi(\mu,l)=\sum_{m=1}^{l-\mu}(mA_m')[(l-m)\Xi(\mu, l-m)]\times\left[\frac{l!}{m!(l-m)!}\right];$$

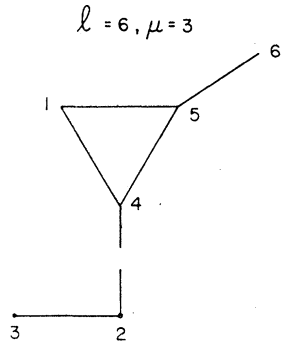

FIG. 6. Example of the breaking of an unlabeled skeleton belonging to Ξ (3,6).

i.e.,

$$\left(1-\frac{\mu}{l}\right)\frac{\Xi(\mu,l)}{(l-1)!}=\sum_{m=1}^{l-\mu}\frac{A_m'}{(m-1)!}\frac{\Xi(\mu, l-m)}{(l-m-1)!}. \quad \text{(III.100)}$$

By introducing the $h(x)$ function defined in (III.96), and the new generating function $H_\mu(x)$ for Ξ:

$$H_\mu(x)=\sum_{l=\mu}^{\infty}(l!)^{-1}(-x)^l\Xi(\mu,l), \quad (\mu\geqq 3), \quad \text{(III.101)}$$

one obtains from (III.100) the relation

$$x\frac{d}{dx}H_\mu-\mu H_\mu=-\left(x\frac{dh}{dx}\right)\left(x\frac{dH_\mu}{dx}\right), \quad (\mu\geqq 3). \quad \text{(III.102)}$$

The function $h(x)$ was explicitly found in (III.97) and (III.98). With the aid of these equations, (III.102) can be integrated, resulting in

$$H_\mu=(\text{constant})[D(x)]^\mu, \quad \text{(III.103)}$$

where the constant is independent of x. As $x\to 0$, $D\to x$ and

$$H_\mu\to(\mu!)^{-1}(-x)^\mu\Xi(\mu,\mu)=(2\mu)^{-1}(-x)^\mu, \quad (\mu\geqq 3). \quad \text{(III.104)}$$

With this condition, (III.103) becomes

$$H_\mu=(2\mu)^{-1}[-D(x)]^\mu, \quad (\mu\geqq 3).$$

In other words

$$\sum_{l=\mu}^{\infty}(l!)^{-1}(-x)^l\Xi(\mu,l)=(2\mu)^{-1}[-D(x)]^\mu, \quad (\mu\geqq 3). \quad \text{(III.105)}$$